JTTEE5 8:87-101

Flattening of Droplets and Formation of Splats in Thermal Spraying: A Review of Recent Work—Part 1

V.V. Sobolev and J.M. Guilemany

(Submitted 3 May 1998; in revised form 21 September 1998)

Properties of the coatings developed during thermal spraying are essentially determined by rapid solidification of splats formed as a result of impingement of the melted powder particles onto a substrate surface. The processes of flattening droplets and formation of splats in thermal spraying have been studied intensively during the last two decades. The last review on this topic was published at the end of 1994. Since then many papers have been dedicated to investigating splat formation, taking into account such important issues as roughness of the substrate surface, wetting phenomena, and splashing. This review, consisting of two parts, includes the main results obtained since 1994 and examines the influence of solidification of the lower part of the splat, substrate roughness, wetting at the substrate-coating interface, substrate deformation, oxidation, and splashing on the dynamics of flattening of droplets and the formation of splats. Flattening of composite powder particles, splat-substrate interaction, and development of splat-substrate adhesion and splat porosity are discussed. Part 1 of the review covers the following issues, which significantly influence the droplet flattening and splat formation: droplet solidification during flattening and roughness of the substrate surface, composite morphology of the powder particles, and oxidation processes. The results provide a better understanding of the thermal spray processes to increase their efficiency.

Keywords oxidation, review, solidification, splat formation

1. Introduction

Coating quality obtained during thermal spraying depends greatly on the dynamics of flattening the molten powder particles. During the last two decades this process has been studied intensively by analytical, numerical, and experimental methods (Ref 1).

Flattening of the thermally sprayed particles (droplets) defines the size and the form of splats developed on the substrate and/or on the prior-deposited coating layers. Solidification of a single splat plays an essential role during thermal spraying because it is almost independent of solidification of the other splats. Thus, the structure and properties of a coating can be considered in terms of formation and solidification of the single splats (Ref 1-5).

The principle findings of investigations, which were undertaken earlier and reviewed in Ref 1, are:

- The kinetics of the droplet flattening depend upon the droplet size and the impact velocity.
- Initially, just after impact, inertial effects dominate. The viscous flow effect becomes more important as the droplet spreads, and the influence of the surface energy could become a significant factor toward the end of the spreading process.
- The major part of the kinetic energy of the impinging droplet is dissipated in overcoming the viscous forces of the flowing droplet. Therefore, the analytical results based on this assumption agree very well with the experimental data.
- Solidification of an impinging droplet occurs during its flattening and significantly influences the splat formation.
- The effect of splashing is very important for the development of splats.

During recent years much attention has been given to further investigation of the droplet flattening and splat formation, taking into account different physical processes. Simple analytical formulas, which are necessary for engineering practice to estimate the parameters of the flattening process, were obtained.

The present review deals with the results obtained after the publication of the paper (Ref 1) and covers the following issues that influence droplet flattening and splat formation: roughness of the substrate surface, droplet solidification during flattening, composite morphology of the powder particles, oxidation processes, wetting and surface phenomena, substrate deformation, splashing of the impinging droplets, and splat-substrate interaction.

Better understanding of the previously mentioned processes contributes to an increase in efficiency of the thermal spray applications. The present review consists of two parts. In Part 1 the influence of solidification and substrate roughness, composite morphology of the powder particles and oxidation processes on the flattening of droplets, and the formation of splats in thermal spraying are considered. Part 2 involves analysis of issues such as wetting and surface phenomena, splat-substrate interaction, splashing of the impinging droplets and substrate deformation on the droplet flattening, and splat formation.

V.V. Sobolev and **J.M. Guilemany,** CPT Thermal Spray Centre, Materials Engineering, Dept. Enginyeria Química i Metallúrgia, Universitat de Barcelona, Marti i Franqués, 1 E-08028 Barcelona, Spain.

2. Influence of Solidification and Surface Roughness

The main focus of the papers reviewed in Ref 1 was to analyze droplet flattening onto a smooth surface without taking into account the splat solidification and the surface morphology. However, the surface roughness significantly alters the flattening dynamics (Ref 6-10), as does the surface-splat friction (Ref 9, 10). The droplet solidification also influences markedly the droplet flattening (Ref 1, 11-14). The droplet mass loss during impingement due to splashing must also be taken into account (Ref 1, 8-10, 14).

In Ref 7 several types of an idealized rough surface were considered, and the two parameters characterizing roughness and its influence on the flattening process were introduced, that is, (a) volume of the valley space corresponding to a unit area of the surface and (b) flowability of a spreading droplet in the valley of the rough surface. With an averaging of the droplet flow, the formulas for the splat diameter and the time of flattening were obtained. It was shown that the ratio of the splat diameter, D, to that of the droplet, d_p, could be approximately presented as $D/d_p = 1.06Re^{1/6}$, where Re is the Reynolds number. In Ref 7, solidification of the flattening droplet was not taken into account.

Nomenclature

a_L	Relative volume of oxidation in splat
a_S	Solid phase thermal diffusivity, m^2/s
b	Splat thickness, m
d_p	Particle diameter, m
D	Splat diameter, m
D_o	Coefficient of diffusion of oxygen, m^2/s
D_{mv}	Dynamic component of coefficient of diffusion, m^2/s
D_e	Effective coefficient of diffusion of oxygen, m^2/s
R_P	Particle radius, m
U	Particle (droplet) impact velocity, ms^{-1}
R	Splat radius, m
t	Time, s
r	Radial coordinate, m
f	Friction coefficient
o_1	Dimensionless parameter: $o_1 = R_pV_s/\varepsilon U$
o_2	Dimensionless parameter: $o_2 = R_pV_s/\delta U$
q_p	Latent heat of fusion of the droplet material, J/kg
P	Pressure, N/m^2
V_S	Solidification velocity, m/s
V_{df}	Volume of diffusive layer, m^3
t_S	Characteristic solidification time, s: $t_S = \delta/V_S$
t_c	Characteristic impact time, s: $t_c = R_p/U$
t_r	Characteristic time, s: $t_r = \varepsilon/V_S$
t_{ox}	Characteristic time of oxidation, s
t_p	Characteristic time, s: $t_p = bU^{-1}$
A_p	Dimensionless parameter: $A_p = 1 - \delta_{ox}/\delta_{df}$
A	Liquid phase thermal diffusivity, m^2/s
R_c	Contact thermal resistance, m^2K/W
R_{co}	Contact thermal resistance at the interface, m^2K/W
R_{cp}	Contact thermal resistance of the precipitate layer, m^2K/W
R_1	Layer thermal resistance, m^2K/W
T	Splat temperature, °C
T_S	Substrate temperature, °C
T_{tr}	Transition temperature, °C
m	Mass, kg
q_{mx}	Mass flux, kg/m^2s
S_p	Particle surface area, m^2
Z	Dimensionless parameter: $Z = m_{ox}/m_p$
M	Dimensionless parameter in Eq 28
H	Dimensionless parameter in Eq 29
X	Dimensionless parameter in Eq 33
Re	Reynolds number: $Re = 2R_pU\rho/\mu$
Re_e	Effective Reynolds number: $Re_e = 2R_pU_e\rho/\mu_e$

Greek symbols

α	Dimensionless parameter: $\alpha = \varepsilon/R_p$
α_C	Contact heat transfer coefficient at the splat-substrate interface, W/m^2K
β	Dimensionless parameter: $\beta = V_S/U$
δ	Thickness of splat lower part, m
δ_1	Layer thickness, m
ΔP	Increment of pressure, N/m^2
ε	Roughness size, m
ζ	Dimensionless splat thicknes: $\zeta = b/R_p$
θ	Dimensionless time: $\theta = UR_p^{-1}t$
λ_1	Layer thermal conductivity, W/mK
μ	Droplet dynamic viscosity, Ns/m^2
ξ	Dimensionless splat radius: $\xi = R/R_p$
ρ	Droplet density, kg/m^3
ρ_L	Liquid phase density, kg/m^3
ρ_S	Solid phase density, kg/m^3
ρ_{ox}	Oxide density, kg/m^3
φ	Solid volume fraction
φ_{ox}	Volume fraction of oxidation
χ	Dimensionless parameter of droplet mass loss
ψ	Correction factor
ω	Correction factor
Ω	Correction factor

Subscripts

o	Initial
*	Characteristic
e	Effective
f	Final
p	Particle
ox	Oxidized material
df	Diffusive
m	Maximum

At the same time modeling of the flattening process undertaken in Ref 11, 12 and analytical estimates obtained in Ref 13 within the framework of the Stefan problem show that spreading of the liquid droplet during flattening and solidification cannot be considered separately, and solidification plays an important role in the entire process.

The general approach to the theoretical analysis of the flattening process developed in Ref 15 results in analytical formulas for the flattening characteristics that agree well with the experimental data. This approach has been used in Ref 6, 8 to 10, and 14 to investigate the effect of surface roughness and solidification on the droplet flattening and the splat formation.

2.1 Droplet Flattening

Consider the droplet flattening on two types of surfaces: rough and smooth. Assume at first that a droplet of radius, R_p, and velocity, U, impinges normally onto a rough surface of the substrate or previously deposited coating layer and that it forms a cylindrical splat (disk) of radius, R, and thickness, b, both of which vary with time, t, during flattening (Fig. 1). The rough surface is characterized by the roughness parameter, α, which is equal to the ratio of the roughness height, ε, to the particle radius: $\alpha = \varepsilon R_p^{-1}$.

Flattening and cooling begin immediately after droplet impingement. The main cooling is caused by heat removal from the lower part of the splat adjacent to the substrate (Ref 16-18). This heat removal depends essentially on the initial temperatures and the thermophysical properties of the substrate and the splat and also on the contact thermal resistance at the substrate-splat interface. The heat removal to the substrate exceeds considerably the heat removal from the upper surface of the splat to the surrounding gas atmosphere (Ref 16-18).

The solidification front moves from the interface with a velocity, V_s, to the interior of the splat. The values of V_s can be determined by the methods described elsewhere (Ref 16, 19). The solidified region of the splat gradually decreases the overall surface roughness and will remove it completely at the time $t_r = \varepsilon V_s^{-1}$. The degree of influence of the splat solidification on the surface roughness is defined by the ratio, o_1, of the impact time , $t_c = R_p U^{-1}$ to t_r (Ref 6):

$$o_1 = R_p V_s / \varepsilon U \qquad \text{(Eq 1)}$$

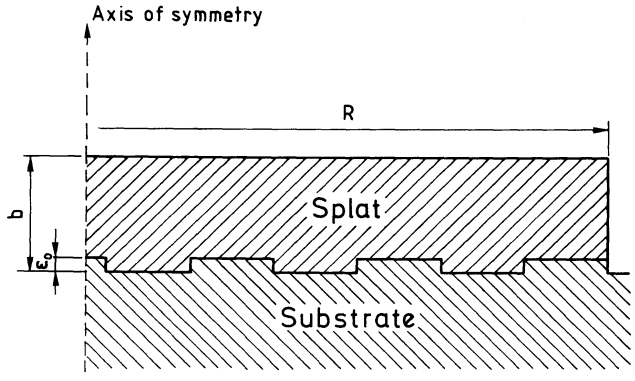

Fig. 1 Schematics of a droplet impingement at a substrate surface

For the flattening process, the important characteristic is solidification of the lower part of the splat with the thickness, δ. Then the characteristic time of solidification is $t_s = V_s^{-1}\delta$. The ratio, o_2, of the impact time, t_c, to t_s is:

$$o_2 = R_p V_s / \delta U \qquad \text{(Eq 2)}$$

When $\delta = \varepsilon$, Eq 2 becomes the same as Eq 1. The ratio β of the solidification velocity, V_S, to that of the droplet impact, U, is also an important parameter of the flattening process:

$$\beta = V_s / U \qquad \text{(Eq 3)}$$

From Eq 1 and 3:

$$o_1 = \beta / \alpha \qquad \text{(Eq 4)}$$

For example, in the case of the plasma spraying of a metallic powder onto an aluminum alloy substrate when $R_p = 20$ μm, $V_s = 5$ ms^{-1}, $\delta = 1$ μm, and $U = 100$ ms^{-1}, then from Eq 2, $o_1 = 1$. Thus, generally, splat solidification must be taken into account when splat flattening is considered. In the particular cases when, for example, the impact velocities, U are high ($U = 800$ ms^{-1}) and the solidification velocities, V_s, are relatively small ($V_s = 0.5$ ms^{-1}), splat solidification could be considered in some approximation to occur after completion of the flattening process (Ref 1, 7, 20). This situation would correspond to high velocity oxygen fuel (HVOF) spraying of the alumina particles. But this separation of flattening and solidification must be treated very carefully because solidification of the lower part of the splat, even though the thickness of the solidified layer is very small, influences significantly the dynamics of the flattening process (Ref 11-14).

Splat solidification may be slowed by the contact thermal resistance at the substrate-splat interface and by the time delay for nucleation of a solid as the crystalline structure is developed (Ref 1, 21, 22). The contact thermal resistance decreases the solidification velocity, V_s, which still remains high (Ref 16, 18). The ratio, N, of the nucleation time to the impact time in the case of homogeneous nucleation was estimated to be large for thermal spray applications (Ref 1, 22). In reality, homogeneous nucleation is unlikely to occur during thermal spraying because of the presence of the inclusions and solid phases (carbides, oxides, etc.) in the impinging droplet. It is also possible that partial solidification of the droplet occurs before impingement (Ref 1, 21). The parameter, N, is usually assumed to be significantly smaller than unity (Ref 1, 6, 8-10). Hence, the delays in nucleation have no practical influence on solidification of the lower part of the splat during flattening.

The impingement process is often associated with the loss of some part of the droplet mass due to splashing and partial rebounding of the droplets during impingement onto the substrate (Ref 1). This mass loss can be characterized by the ratio, χ, of the droplet mass, which remains after these events to the initial mass of the impinging droplet (Ref 6, 8-10).

2.2 Surface Roughness

To take into account the surface roughness during the flattening process, it is assumed that roughness increases the value of the shear stress because of the friction between a flattening

droplet and the rough surface. Assuming that the flow is turbulent,the Blench formula can be used for assessing the friction coefficient, f (Ref 23):

$$f = 0.79\alpha^{1/2} \quad \text{(Eq 5)}$$

In Ref 6 the roughness, ε, is considered to change during the splat solidification according to the formula:

$$\varepsilon = \varepsilon_o - V_s t \quad \text{(Eq 6)}$$

For simplicity, the rough surface is assumed to consist of the rectangular "teeth" of the height, ε (Ref 6). Their height is assumed to be equal to the distance between them (Fig. 1). Then, the variation of the splat thickness, b, due to the surface roughness can be taken as $b - 0.5\varepsilon$. By taking into account splat solidification and droplet mass loss, the mass conservation condition can be written as:

$$4\chi R_p^3/3 = R^2(b - 0.5\varepsilon - V_s t) \quad \text{(Eq 7)}$$

From Eq 7 the following equation for the splat radius, R, is:

$$R = 2R_p(\chi R_p/3)^{1/2}(b - 0.5\varepsilon - V_s t) \quad \text{(Eq 8)}$$

In the case of a smooth surface, the friction between it and the splat can be described by the following coefficient of friction, f (Ref 23):

$$f = 0.316Re^{-0.25} \quad \text{(Eq 9)}$$

Transient characteristics of the droplet flattening on a rough surface were obtained in Ref 6, based upon the previous equations. They include analytical formulas describing variations of the dimensionless splat thickness, $\zeta = b/R_p$; the dimensionless splat radius, $\xi = R/R_p$; and the rate parameters, $d\zeta/d\theta$ and $d\xi/d\theta$, with the dimensionless time, $\theta = UR_p^{-1}t$, for a typical thermal spray situation when $Re >> 1$ (Ref 6, 8-10). It follows from these formulas that an increase in the surface roughness causes an increase in the splat thickness and a decrease in the splat radius as well as a decrease in $d\xi/d\theta$ and the absolute value of $d\zeta/d\theta$. The splat solidification leads to a decrease in ζ and an increase in ξ. It also causes an increase in $d\xi/d\theta$ and in the absolute value of $d\zeta/d\theta$.

Similar formulas were obtained for a droplet flattening on a smooth surface. It follows that an increase in the surface-splat friction during the flattening process causes the same qualitative variations of ζ, ξ, $d\zeta/d\theta$, and $d\xi/d\theta$ as an increase in the surface roughness. The analytical results obtained are valid up to $t < t_*$, where (Ref 15):

$$t_* = 1.25R_p U^{-1} \ln(1 + 0.3Re) \quad \text{(Eq 10)}$$

The value of t_* is greater than the characteristic time of flattening, and the analytical results obtained are valid for the whole time interval for droplet flattening.

The final values of ζ_f and ξ_f are determined by the formulas (Ref 6, 8-10):

$$\zeta_f = 1.826Re^{-1/2}[1 + 0.12\alpha^{1/2}Re^{1/2} - 0.68\beta Re^{1/2}\ln(0.3Re)] \quad \text{(Eq 11)}$$

$$\xi_f = 0.8546\chi^{1/2}Re^{1/4}[1 - 0.06\alpha^{1/2}Re^{1/2} + 0.34\beta Re^{1/2}\ln(0.3Re)] \quad \text{(Eq 12)}$$

Similar formulas were obtained in the case of a smooth surface with surface-splat friction (Ref 8-10). From Eq 11 it follows that the final splat thickness decreases with an increase in the Reynolds number. This thickness increases with an increase in the surface roughness and decreases with an increase in the solidification velocity. The final splat radius (Eq 12) generally varies nonuniformly with the Reynolds number. First it increases, achieves a maximum value, and then decreases. The final value of ξ diminishes when the surface roughness and the mass loss are increased. The parameter, ξ_f, increases with an increase in the splat solidification velocity.

The results obtained in Ref 6 show that the absolute value of the final rate parameter, $d\zeta_f/d\theta$, decreases with an increase in the surface roughness when the splat solidification is not taken into account ($\beta = 0$). This value increases with an increase in α when the splat solidification causes an increase in the absolute value of, $d\zeta_f/d\theta$. The rate parameter, $d\xi_f/d\theta$, decreases when the surface roughness and the droplet mass loss increase. Splat solidification gives rise to an increase in, $d\xi_f/d\theta$.

In the case of a smooth surface ($\alpha = 0$,) the influence of the surface-splat friction on the final characteristics of the flattening is similar to the influence of the surface roughness.

When splat solidification is absent ($\beta = 0$), the influence of the surface roughness on the flattening process is shown to be equivalent to the influence of an effective viscosity, μ_e, which is approximately (Ref 6):

$$\mu_e = \mu(1 + 0.24\alpha^{1/2}Re^{1/2}) \quad \text{(Eq 13)}$$

It can be shown that the influence of the surface-splat friction on the flattening at a smooth surface in the absence of splat solidification is equivalent to the influence of an effective viscosity, $\mu_e = 1.16\ \mu$. For flattening at a smooth surface ($\alpha = 0$) without surface-splat friction, the influence of the splat solidification is equivalent to the influence of an effective velocity, U_e, of the droplet impingement, which is approximately (Ref 15):

$$U_e = U[1 + 0.34\beta Re^{1/2}\ln(0.3Re)] \quad \text{(Eq 14)}$$

Thus, it can be shown that droplet flattening at a rough surface with splat solidification is equivalent to flattening at the smooth surface without splat solidification and without surface-splat friction, under conditions when the velocity of droplet impingement is U_e and the dynamic viscosity of the droplet liquid phase is μ_e. Under these conditions, Eq 11 and 12 can be written as:

$$\zeta_f = 1.826\,Re_e^{1/2} \quad Re_e = 2RU_e\rho/\mu_e \quad \text{(Eq 15)}$$

$$\xi_f = 0.8546\,\chi^{1/2}Re_e^{1/4} \quad \text{(Eq 16)}$$

The similar formulas can be written for the droplet flattening at a smooth surface with surface-splat friction.

Experimental values of the final splat radius, ξ_f, obtained during the plasma spraying of the zirconia particles onto a steel

substrate (Ref 24, 25) have been used to compare the analytical and experimental data.

First, consider the experimental data corresponding to the flattening at a smooth steel substrate (Ref 25). In this case the solidification velocity can be approximated as:

$$V_s = \alpha_c T_p/(q_p \rho) \quad \text{(Eq 17)}$$

where α_c is the contact heat transfer coefficient at the splat-substrate interface, T_p is the droplet temperature, and q_p is the latent heat of fusion of the droplet material. The average particle temperature T_p was about 3660 K (Ref 25). Taking $q_p = 0.71 \times 10^6$ Jkg^{-1}, $\rho = 5400$ kgm^{-3}, and $\alpha_c = 3.8 \times 10^5$ $Wm^{-2}K^{-1}$, from Eq 17, $V_s = 0.366$ ms^{-1}. Taking the impact velocity, $U = 150$ ms^{-1} (Ref 25), $\beta = 0.00244$ is obtained.

Using this value of β and assuming that there is no mass loss from the droplet ($\chi = 1$) because the substrate is heated and its surface is smooth (Ref 25), the analytical results given in Ref 8 and 10 (when the surface-splat friction is negligible), indicate the variation of the splat final radius (flattening degree), ξ_f, with the Reynolds number, *Re*. Figure 2 shows this variation together with the experimental data and their correlation. The theoretical values of ξ_f agree well with the experimental data.

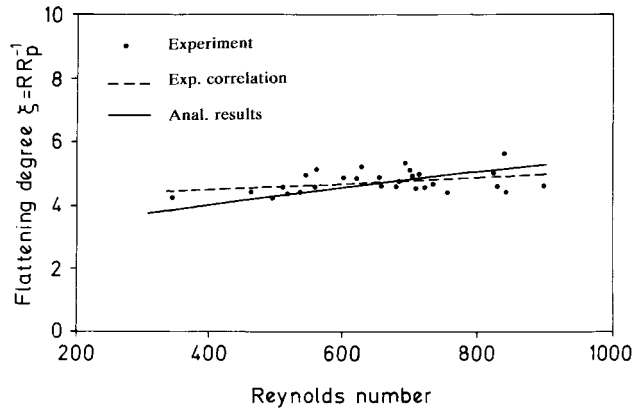

Fig. 2 Comparison of analytical and experimental results describing the final splat radius on a smooth substrate. Experimental results are from Ref 25. After Ref 6

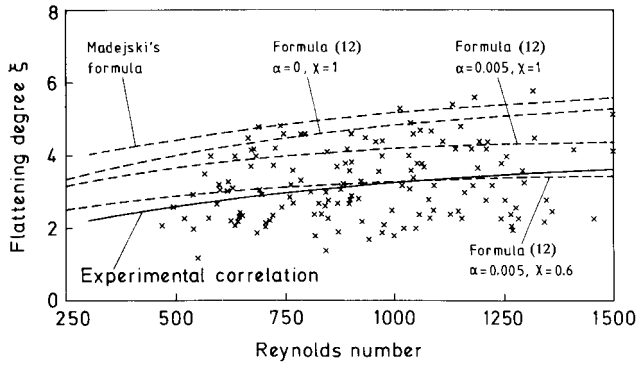

Fig. 3 Comparison of the analytical and experimental results describing the final splat radius (flattening degree) on a rough substrate. x, experimental results from Ref 24. After Ref 6

In Ref 24 the degree of flattening was measured for a rough steel substrate. In the case of the zirconia particles, the solidification velocity was small due to the low thermal diffusivity of this material. Hence the third term at the right hand side of Eq 12 for ξ_f may be neglected in comparison to the second term. In this case the substrate can be considered to be relatively "cold" because its temperature is only 75 °C. Thus, the droplet mass loss due to splashing should be more pronounced and have more influence on the flattening process.

The theoretical curves in Fig. 3 obtained from Eq 12 show that when surface roughness and mass loss from the droplet are taken into account, then the theoretical results fit markedly better with the experimental data than when these factors are not taken into account (Ref 24).

3. Flattening of Composite Powder Particles

Composite powders such as WC-Co, WC-Co-Cr, Cr_3O_2-NiCr, etc., play an essential role in production of wear and corrosion resistant thermally sprayed coatings. Therefore, an analysis of the flattening process of these particles is industrially important. Analytical investigation of this process was undertaken in Ref 20. In Ref 26 experimental data were obtained on the flattening of WC-Co powder particles.

Consider an agglomerate composite particle consisting of small high melting point solid components (e.g., carbides) and a binding metal. Assume that during thermal spraying the binder melts and the solid components are markedly smaller than the splat thickness and the surface roughness, ε_0, and a liquid-solid mixture of the impinging droplet can be considered as a quasi-homogeneous medium with a solid volume fraction, φ_1.

Because there is no great difference between the densities of liquid and solid phases of the droplet, it is reasonable to assume that the relative movement between these phases is negligible in the bulk volume of the splat and, therefore, the interaction forces between them can be neglected (Ref 27). With the small value of φ_1, the liquid-solid mixture of the droplet can be considered as a uniform medium with the effective dynamic viscosity μ_e (Ref 28):

$$\mu_e = \mu(1 - \varphi_1)^{-1} \quad \text{(Eq 18)}$$

From Eq 18 it is seen that the presence of the solid phase increases the flow viscosity. It also occurs due to the non-Newtonian character of the liquid-solid flow, which becomes more pronounced under the temperatures near the solidification point (Ref 28, 29). During flattening, the spreading flow is turbulent, and at the droplet-substrate interface, friction decreases in comparison with a single phase flow because of reduced mixing length due to dissipation by the solid particles (Ref 28).

To take into account the roughness, ε, of the substrate surface during the flattening process, assume that it increases the shear stress by the value that arises because of friction between a flattening droplet and the rough surface. Following Ref 6, a modified Blench formula (Eq 5) is used for the friction coefficient, *f*, with a correction factor, ω, accounting for a decrease in friction in the liquid-solid flow: $f = 0.079\omega\alpha^{1/2}$.

In the case of the smooth surface, the friction coefficient can be described by a similar equation with the correction factor, ω. The liquid-solid splat solidification velocity depends on the thermophysical properties of the liquid and solid phases and the contact heat transfer coefficient, α_C, at the splat-substrate interface. If the thermal diffusivity of the solid (e.g., carbide WC) a_S is greater than that of liquid a_L (metallic binder); this contributes to an increase in the rate of heat transfer inside of the splat. But an increase in V_S would hardly ever occur because of the relatively large contact thermal resistance at the interface (Ref 1).

The most important case is when the thermal diffusivity of the solid (e.g., oxide) is less than that of the liquid phase. Then the heat transfer rate inside the splat decreases. This decrease can be more pronounced when the solid density, ρ_S, exceeds that of the liquid phase and solid particles precipitate in the lower part of the splat. The surface roughness contributes to precipitation because the solid particles can be precipitated in the wavy structure of the rough surface.

The characteristic time of precipitation, t_P, is approximately equal to bU^{-1} (Ref 30). Roughness will be important during precipitation of solids if it is not covered by the solidification front moving with the velocity, V_S. This front will cover the surface roughness completely at the time, t_S Therefore, the degree of roughness influence on the precipitation process is determined by the ratio, Ω, of the time, t_P, to t_S, that is, $\Omega = bV_S/\varepsilon U$.

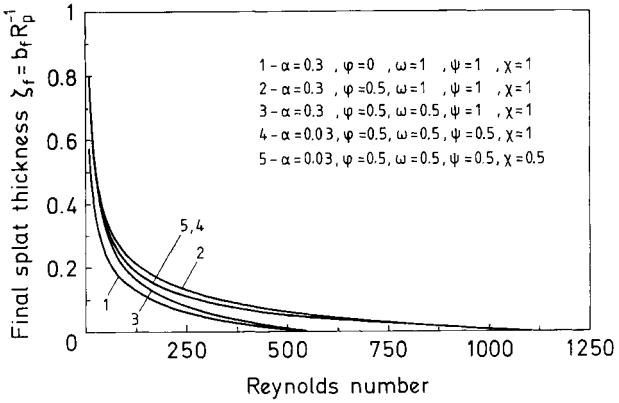

Fig. 4 Variation of final splat thickness with Reynolds number for the rough surface. After Ref 20

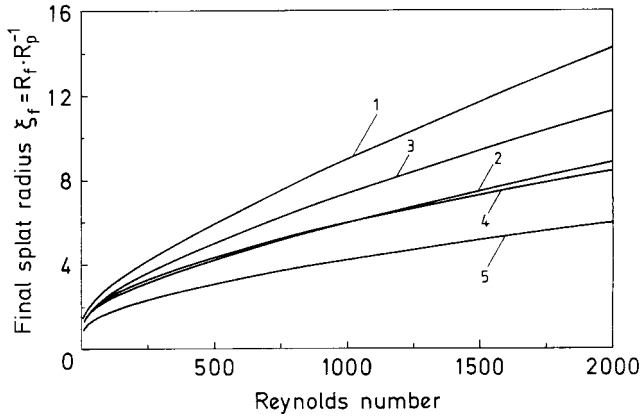

Fig. 5 Variation of final splat radius with Reynolds number for the rough surface. After Ref 20

Because the splat thickness, b, is of the same order of magnitude as the initial surface roughness, ε_0, and the droplet impinging velocity, U, is much greater than V_S, the value $\Omega << 1$ in the thermal spray applications. Therefore, surface roughness plays an important role in the precipitation of solids.

When $a_S < a_L$ and $\rho_S > \rho_L$, the precipitation of solids can lead to an increase in the contact thermal resistance, R_C, at the interface. This occurs if the thermal resistance, R_{CP}, of the precipitate layer of solid is greater than the thermal resistance, R_{CO}, at the interface when the solid phase is absent ($\varphi_1 = 0$) or is comparable to it.

Consider an example of HVOF spraying of the Cr_3C_2-NiCr powder onto a steel substrate. An impinging molten droplet consists of the solid phase including different chromium carbides, chrome oxide Cr_2O_3, and a liquid phase of Cr-Ni-C, formed due to in-flight dissolution of Cr_3C_2 (Ref 31). The most critical factor for the contact thermal resistance is the precipitation of the chromium oxide, which has a low thermal conductivity λ_1.

The thermal resistance, R_1, of the layer of Cr_2O_3 with the thickness, δ_1, is equal to $\delta_1\lambda_1^{-1}$. Assume that the rough substrate surface consists of rectangular "teeth" with the initial height, ε_0, and length equal to the distance between them. Then, the value of δ_1 can be taken as $0.5\varepsilon_0$. When the value of $\delta_1 = 2$ μm and $\lambda_1 = 20$ $Wm^{-1}K^{-1}$, $R_1 = 10^{-7}$ $W^{-1}m^2K$. This value of R_1 can be comparable with R_{CO} and even exceed it (Ref 21). Therefore, in this case the presence of the solid phase in the splat leads to an increase in the contact thermal resistance at the splat-substrate interface and to a decrease in the solidification velocity, V_S.

The solidification velocity can be calculated from Eq 17. To take into account the solidification process during flattening of the composite droplets, it is worth introducing the solidification velocity, V_{Se}, with a correction factor, ψ, which accounts for the changes in V_S associated with the solid phase of the droplet, $V_{Se} = \psi V_S$. Then $\beta_e = V_{Se}/U$. The most probable situation corresponds to $\psi < 1$.

In the case of the droplet flattening on the rough surface using the results of Ref 20, the following formulas can be obtained for the flattening characteristics when $Re_* >> 1$:

$$\zeta_f = 1.826\, Re_e^{-1/2}[1 + 0.12\,\omega\alpha^{1/2}Re_e^{1/2} - 0.68\,\beta_e Re_e^{1/2}\ln(0.3\,Re_e)] \quad \text{(Eq 19)}$$

$$\xi_f = 0.8546\,\chi^{1/2}\,Re_e^{1/4}[1 - 0.06\,\omega\alpha^{1/2}Re_e^{1/2} + 0.34\,\beta_e Re_e^{1/2}\ln(0.3\,Re_e)] \quad \text{(Eq 20)}$$

It follows from Eq 19 and 20 and the results of Ref 20 that, without taking into account the surface roughness ($\alpha = 0$) and the splat solidification ($\beta_e = 0$), the presence of the solid particles in the flattening droplet ($\varphi_1 \neq 0$) leads to (a) an increase in the final splat thickness and the final absolute value of $d\zeta_f/d\theta$,and (b) a decrease in the final splat radius, ξ_f, and the rate parameter, $d\xi_f/d\theta$, in comparison with the homogeneous droplet ($\varphi_1 = 0$). This occurs because of the additional energy dissipation caused by the solid phase. When $\varphi_1 \neq 0$, the contributions of the surface roughness and the splat solidification to the flattening characteristics are less pronounced than in the case when $\varphi_1 = 0$. Their relative contributions depend on the specific values of

φ_1, ω, and ψ. The formulas similar to Eq 19 and 20 are also established in the case of flattening on the smooth surface (Ref 8-10).

Use of analytical expressions, Eq 19 and 20, shows that, in the absence of the splat solidification ($\beta_e = 0$), the influence of the surface roughness is equivalent to the influence of a characteristic effective viscosity μ_{*e}:$\mu_{*e} = \mu_e(1 + 0.24\omega\alpha^{1/2}Re_e^{1/2})$. For the flattening at a smooth surface ($\alpha = 0$) without splat-surface friction, the influence of the splat solidification is equivalent to the influence of a characteristic effective velocity, U_{*e}, of the droplet impingement. From Eq 19 and 20, it follows that the value of μ_e is $U_{*e} = U[1 + 0.34\beta_e Re_e^{1/2} \ln (0.3Re_e)]^4$.

Using Eq 19 and 20, it can be shown that the liquid-solid droplet flattening at a rough surface with splat solidification is equivalent to the flattening at the smooth surface without splat solidification and with negligible influence of splat-surface friction, under conditions when the velocity of droplet impingement is μ_{*e} and the dynamic viscosity of the droplet is μ_{*e} Under these conditions Eq 19 and 20 can be written in the form:

$$\zeta_f = 1.826\, Re_{*e}^{-1/2} \qquad Re_{*e} = 2R_p\mu_{*e}\rho/\mu_{*e} \qquad \text{(Eq 21)}$$

$$\xi_f = 0.8546\, \chi^{1/2} Re_{*e}^{1/4} \qquad \text{(Eq 22)}$$

For thermal spray practice it is important to know the variations of the final parameters of flattening. In the case of a rough surface, the numerical analysis of Eq 19 and 20 when $\beta = 0.03$ gives the curves shown in Fig. 4 and 5. The final splat thickness decreases with an increase in the Reynolds number (Fig. 4). The value of ζ_f undergoes an increase with an increase in φ_1 and ω. The final splat thickness increases when ψ decreases. Figure 5 shows that the final splat radius decreases with an increase in φ_1 and ω. The value of ξ_f increases when χ and ψ increase.

Smooth surface results are in the curves shown in Fig. 6 and 7. The final value of the splat thickness decreases with a decrease in ω and varies nonuniformly, attaining the minimum at the small Reynolds numbers (Fig. 6). An increase in φ_1 gives rise to ζ_f at the small *Re* and causes a decrease of ζ_f with the further increase in *Re*. When ψ decreases, the value of ζ_f enhances. Figure 7 shows that the final splat radius increases with a decrease in ω. An increase in χ and ψ leads to an increase in ξ_f. The value of ξ_f decreases when φ_1 enhances.

The effect of WC particle size on the flattening of WC-Co splats during HVOF spraying was studied experimentally in (Ref 26). Four types of WC-Co powders were considered: sintered-crushed (type 1 and 2), agglomerated (type 3), and coated (type 4).

Equation 19 is used to calculate the final value $\zeta_f = bR_p^{-1}$ of the splat thickness when the splat solidification is considered negligible (Ref 26). Assume that ρ = 14,900 kgm^{-3}, $\mu = 3.10^{-3}$ kg(ms)$^{-1}$, $\omega = 0.9$, $\varphi_1 = 0.3$, and $\alpha = 0.5$. For powder type 1 consider U = 325 ms^{-1}, and for types 2 and 3 U = 190 ms^{-1} (Ref 26). Then, for the different values of the particle diameter, d_p, the calculated values of the ratio $d_P b^{-1}$ are shown in the Table 1. It can be seen that the theoretical results agree well with the experimental data.

4. Influence of Oxidation on Splat Formation

Oxidation of coatings during thermal spraying essentially influences their structure and properties (Ref 2, 32-37). Due to the difference in the expansion coefficients of metallic and oxide phases, the metallic coatings containing oxide phases may be subjected to irregular degradation during thermal cycling (Ref 32). Generally, the coatings with oxides seem to be more difficult to machine and exhibit less ductility in service (Ref 35). For the wear resistant carbide based coatings, it is important to avoid a loss of carbides due to oxidation during spraying. Otherwise

Table 1 Comparison of the theoretical and experimental results

Coatings	b, μm	d_p, μm	d_P/b Calculated	d_P/b Experimental
Type 1	2.27 ± 0.95	20	12.89	6.21-15.15
Type 2	2.37 ± 0.95	38	13.07	11.45-26.76
Type 3	2.93 ± 0.95	40	13.10	10.31-20.20

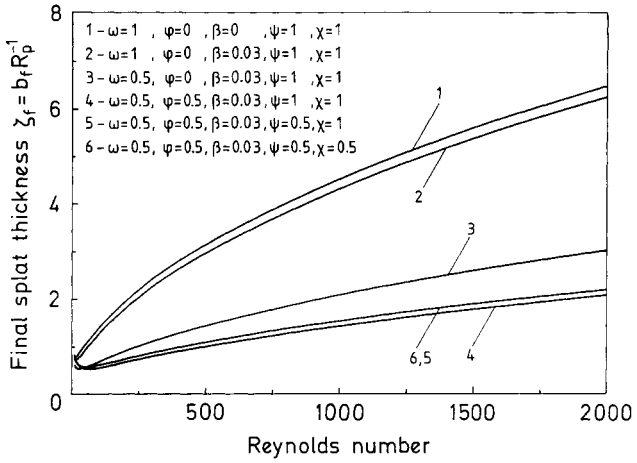

Fig. 6 Variation of final splat thickness with Reynolds number for the smooth surface. After Ref 20

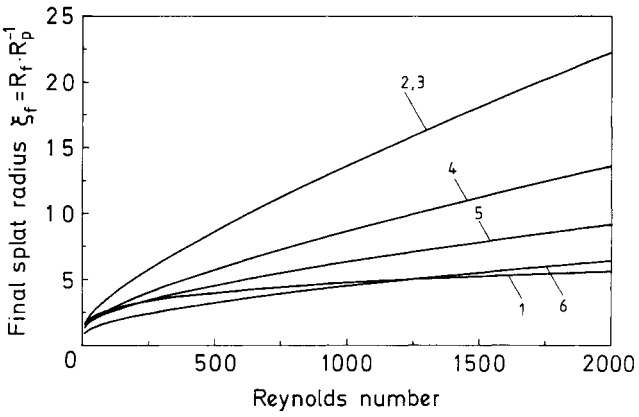

Fig. 7 Variation of final splat radius with Reynolds number for the smooth surface. After Ref 20

these coatings will not be sufficiently wear resistant for use in industrial applications (Ref 34).

In Ref 36 it was shown that oxidation directly affects hardness and wear performance. The properties of the corrosion resistant coatings often depend on the levels of their oxidation (Ref 33). High temperature oxidation is a major concern in gas turbines today because at temperatures above approximately 870 °C, relatively rapid oxidation can occur unless there is a barrier to oxygen diffusion on the surface of the component (Ref 36). However, many currently used high strength alloys do not develop sufficiently protective barriers because their chemical compositions have been optimized for high temperature strength and metallurgical stability rather than for oxidation resistance (Ref 36).

Oxidation influences the different processes involved in the development of the coating. Particularly, it has a noticeable influence upon the droplet flattening and the splat-substrate interactions, which are important for the coating formation (Ref 27, 31, 38-40). The presence of dissolved oxygen in a solidifying splat affects the splat-substrate wetting, which in turn influences the flattening process.

The coating structure obtained as a result of the HVOF spraying of the Cr_3C_2-NiCr powder onto a mild steel substrate shows that the main oxidation of chromium and the formation of Cr_2O_3 seem to take place during the in-flight motion of the powder particles (Ref 39). According to the results presented in Ref 35, the main oxidation of the coatings obtained during the HVOF spraying of aluminum takes place at the substrate surface where the coatings are exposed to an oxygen-rich boundary layer, which envelops the surface of the substrate.

This section involves investigation of the effect of oxidation on the dynamics of flattening of powder particles and the development of the splat-substrate interactions during thermal spraying and presents analytical formulas that permit estimation of these processes during practice (Ref 40). The analytical results take into account the roughness of the substrate, the splat solidification, wetting, splashing, and the place where oxidation occurs during the in-flight motion of the powder particles and/or exposure of the solidifying splat to the surrounding oxygen-rich atmosphere at the substrate surface.

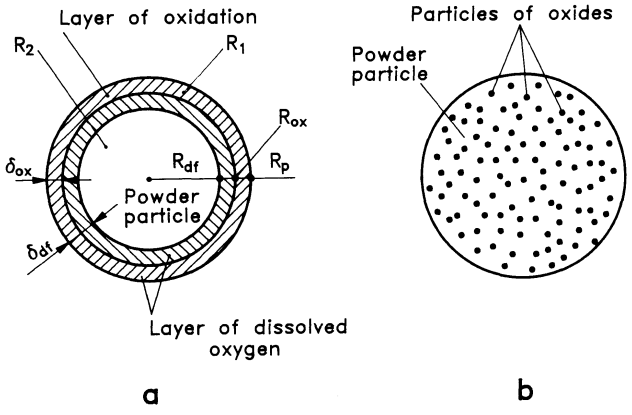

Fig. 8 Development of layers of oxides and dissolved oxygen in the powder particle during its (a) in-flight motion and (b) mixing of the oxides in the bulk volume of the particle due to turbulence of the surrounding gases

4.1 In-Flight Oxidation

Due to the high temperatures of the surrounding gases during thermal spraying, the powder particles are usually melted at the spray distance and the liquid phase, which appears to react with oxygen. Conditions for the coating oxidation are rather favorable in the case of the HVOF spraying because the combustion products contain excessive oxygen (with respect to the stoichiometric ratio).

Two mass transfer processes can take place during interaction of the liquid particle with oxygen: (a) development of oxides due to chemical reactions between the surface of the liquid phase and oxygen and (b) diffusion of oxygen in the liquid. The rate of the formation of oxides can be estimated according to (Ref 38).

The mass of an oxidation layer developed m_{ox} can be presented as $m_{ox} = q_{ms}S_p t_{ox}$, where q_{ms} is the mass flux of the oxide, S_p is the surface area of the particle subjected to oxidation, and t_{ox} is the characteristic time of oxidation. The ratio Z of m_{ox} to the particle mass $m_p = 4\pi R_p^3\rho/3$ is:

$$Z = 3q_{ms}t_{ox}(\rho R_p)^{-1} \quad \text{(Eq 23)}$$

The value of Z can be considered as the relative mass of oxidation giving the level of oxidation. The thickness, δ_{ox}, of the oxidized layer, which is equal to the difference between the particle radius, R_p, and the radius of the inferior boundary of the oxidized region, R_{ox} ($\delta_{ox} = R_p - R_{ox}$, Fig. 8) can be presented as:

$$\delta_{ox} = R_p[1 - (1 - Z\rho\rho_{ox}^{-1})^{1/3}] \quad \text{(Eq 24)}$$

where ρ_{ox} is the oxide density. When $Z << 1$ from Eq 24, it follows that the thickness, δ_{ox}, can be estimated by the formula $\delta_{ox} = Z\rho R_p(3\rho_{ox})^{-1}$.

Consider, for example, HVOF spraying of the Cr_3C_2-NiCr powder when Cr_2O_3 oxide is formed during the particle flight (Ref 39). To provide estimations, assume that the oxide mass flux, q_{ms}, in this case has a value similar to that corresponding to the development of the FeO oxide when an iron droplet is oxidized (Ref 38) and $q_{ms} = 3.6 kg/(m^2 s)$. The value of the characteristic time of oxidation, t_{ox}, can be taken as equal to the characteristic time of the particle flight during thermal spraying, which is approximately 1 ms (Ref 9, 31, 38). Taking ρ =7500 kgm^{-3}, ρ_{ox} =5210 kgm^{-3}, and R_p = 20 μm, from Eq 23 and 24, it is found that Z = 0.072 (7.2%) and δ_{ox} = 0.716 μm (716 nm). When R_p = 10 μm, Z = 0.144 (14.4%) and δ_{ox} = 0.745 μm (745 nm). It is seen that a decrease in the particle radius leads to an increase in the level of oxidation, Z, and the thickness of the oxidized layer, δ_{ox}. An increase in Z is more pronounced than that in δ_{ox}.

It is convenient to introduce the volume fraction of oxidation, φ_{ox}, in the following manner. The thickness of the layer of oxidation, δ_{ox}, is equal to the difference between the radius of the particle, R_p, and the value of R_{ox} (Fig. 8): $\delta_{ox} = R_p - R_{ox}$. The volume fraction of the oxides, φ_{ox}, formed in the particle is equal to the ratio of the volume of the the oxidized layer, V_{ox}, to the volume of the particle, V_p. Taking into account that $V_p = 4\pi R_p^3/3$ and $V_{ox} = 4\pi(R_p^3 - R_{ox}^3)/3$, then the expression for the value of δ_{ox} is:

$$\delta_{ox} = R_p[1 - (1 - \varphi_{ox})^{1/3}] \quad \text{(Eq 25)}$$

Taking into account that the volume of oxidation, V_{ox}, is equal to the volume of the spherical layer with the thickness δ_{ox}: $V_{ox} = 4\pi R_p^2 \delta_{ox}$, then the volume fraction of oxidation, φ_{ox}, can be presented as:

$$\varphi_{ox} = 3\delta_{ox} R_p^{-1} \quad \text{(Eq 26)}$$

It is seen that the relative volume of oxidation, φ_{ox} (as the relative mass of oxidation, Z), increases with a decrease in the particle radius. If the value of R_p for the Cr_3C_2-NiCr powder varies from 10 to 40 μm, the value of φ_{ox} changes from 22 to 5%. Therefore, in order to decrease the in-flight oxidation, it is necessary to have a narrow size distribution of the powder particles with a relatively large mean value.

Diffusion of oxygen occurs in the surface layer with the thickness, δ_{fl}, of a melted powder particle of the radius, R_p. Intensive turbulent motion of the surrounding gases can cause a motion of the liquid phase in this layer. As a result, the coefficient of diffusion, D_o, of oxygen in the liquid phase of the particle increases by the value of D_{mv} associated with the liquid motion. Then, the thickness of the diffusive layer, δ_{fl}, can be estimated using the effective coefficient of diffusion of oxygen, D_e, by the formula:

$$\delta_{fl} = (D_e t_{fl})^{1/2} \quad D_e = D_o + D_{mv} \quad \text{(Eq 27)}$$

where t_{fl} is the time interval between starting of particle melting and its impingement onto the substrate. If particle solidification occurs at the spraying distance, then the value of t_{fl} is equal to the difference between the finishing time of the solidification process and the starting time of the particle melting. With a decrease in R_p, the value of t_{fl} approaches the time of the particle flight at the spray distance.

In the case of intensive motion of the liquid phase, the value of D_{mv} can exceed significantly the coefficient of diffusion, D_o (Ref 41). During HVOF spraying of the composite powder, particles consisting of, for example, carbides and a metallic binder, the velocity of the liquid phase decreases because the carbides increase the effective viscosity of the liquid-solid mixture, which arises after melting of the binder (Ref 20). This would lead to a decrease in the value of D_{mv} (and, hence, D_e) and to a decrease in the level of the oxygen diffusion in the particle in comparison with the homogeneous particle without carbides.

Taking the typical values of $D_o = 10^{-9} m^2 s^{-1}$ and $t_{fl} = 10^{-3}$ s, from Eq 27 $\delta_{fl} = 1$ μm, when $D_{mv} = 0$. If, for example, $D_{mv} = 3 \times 10^{-9} m^2 s^{-1}$, then from Eq 27 it follows that $\delta_{fl} = 2$ μm. It is seen that the thickness of the layer of the oxygen diffusion, δ_{fl}, markedly exceeds the thickness of the layer of oxidation, δ_{ox}.

It is possible to introduce the relative volume or the volume fraction of the oxygen diffusion, φ_{df}. The thickness of the diffusive layer, δ_{df}, is equal to the difference between the radius of the particle, R_p, and the value of R_{df}: $\delta_{df} = R_p - R_{df}$ (Fig. 8). The volume fraction of the diffusive layer, φ_{df}, developed in the particle due to the diffusion of oxygen is equal to the ratio of the volume of the diffusive layer, V_{df}, to the volume of the particle, V_p. Thus, taking into account that $V_{df} = 4\pi(R_p^3 - R_{df}^3)/3$, the following formulas for δ_{df} and φ_{df} are obtained: $\delta_{df} = R_p[1 - (1 - \varphi_{df})^{1/3}]$ and $\varphi_{df} = 3\delta_{df} R_p^{-1}$.

These formulas are similar to those of Eq 25 and 26 for δ_{ox} and φ_{ox}, respectively. The volume fraction of the oxygen diffusion, φ_{df}, decreases with an increase in the particle radius in a similar manner as the volume fraction of oxidation, φ_{ox}. When R_p varies from 10 to 60 μm, the value of φ_{df} changes from 30 to 5% if $\delta_{df} = 1$ μm and from 60 to 10% if $\delta_{df} = 2$ μm.

It is seen that $\delta_{df} > \delta_{ox}$. The relative difference, A_p, between δ_{df} and δ_{ox} ($A_p = 1 - \delta_{ox}/\delta_{df}$) determines the relative volume of the powder particle where only diffusive (dissolved) oxygen is contained. In the case of HVOF spraying of Cr_3C_2-NiCr powder when $R_p = 20$ μm, the value of $A_p = 28.4\%$ when $\delta_{df} = 1$ μm, and $A_p = 64.2\%$ when $\delta_{df} = 2$ μm.

Consider an influence of oxidation on the heat transfer between the particle and the surrounding gases. This heat transfer depends on the thermal resistancem, R_{pr}, of the powder particle, which is equal to the sum of the thermal resistances of the oxidized layer, R_1, and that of the rest of the particle , R_2 (Fig. 8a): $R_{pr} = R_1 + R_2$, $R_1 = \delta_{ox}\lambda_{ox}^{-1}$, and $R_2 = (R_p - \delta_{ox})\lambda_p^{-1}$, where λ_{ox} and λ_p are the coefficients of thermal conductivity of the oxidized layer and the particle, respectively. The ratio $M = R_1/R_2$ is:

$$M = \lambda_p \varphi_{ox}[3\lambda_{ox}(1 - \varphi_{ox}/3)]^{-1} \quad \text{(Eq 28)}$$

The influence of the thermal resistance, R_1, of the oxidized layer increases with an increase in the particle thermal conductivity, λ_p, and the volume fraction of oxidation, φ_{ox}, and a decrease in the thermal conductivity of the developed oxides, λ_{ox}.

Consider, for example, the HVOF spraying of the Cr_3C_2-NiCr powder onto a mild steel substrate when a chromium oxide Cr_2O_3 is formed during the particle motion at the spray distance (Ref 31, 39). Taking $R_p = 20$ μm, $\lambda_p = 70$ W/(mK), and $\lambda_{ox} = 22$ W/(mK), then from Eq 28 $M = 0.31$ evolves. Thus, in this case the thermal resistance, R_1 of the oxidized layer constitutes about one-third of R_2 of the rest of the particle.

Turbulent mixing of the liquid part of the powder particle during its in-flight motion destroys the surface layer of oxides and causes the oxides to be distributed more uniformly through the bulk volume of the composite particle (Fig. 8b). As the thermal diffusivity of the oxides is significantly less than that of the metallic (or carbide) phase, the presence of oxides in the particle volume decreases the particle thermal diffusivity and, hence, slows down the heat exchange between the particle and the surrounding gases.

Usually the reactions of oxidation are accompanied by heat release. This occurs in the surface layer of the particle and, due to very small thickness of this layer, most heat seems to be transferred outside of the particle. Some part of this heat may be transferred inside the particle and would contribute to particle melting. However, this effect is weakened because of a decrease in the particle thermal diffusivity caused by oxidation.

The oxides developed during particle flight at the spraying distance play an important role in droplet flattening and splat-substrate interaction. Oxidation also takes place at the upper liquid surface of the solidifying splat. This oxidation is considered in the following section.

4.2 Splat Oxidation

During droplet flattening, the upper surface of the forming splat is exposed to the surrounding oxygen-rich atmosphere, and

this leads to oxidation of this surface during the characteristic time of the splat solidification, t_s (Fig. 9a). The process of oxidation is similar to that studied previously for the in-flight oxidation of the powder particle.

Consider the formation of a regular disk splat with radius, R, and thickness, b, as a result of flattening of the droplet with radius, R_p, impinging onto the substrate surface. Using the arguments similar to those given in Ref 40, it is possible to show that the ratio, H, of the mass of the oxidized layer in the splat to the splat mass is determined by the formula:

$$H = q_{ms} t_s (\rho b)^{-1} \quad \text{(Eq 29)}$$

The thickness of an oxidized layer, Δ_{ox}, can be presented in a form:

$$\Delta_{ox} = \rho b H/\rho_{ox} = q_{ms} t_s/\rho_{ox} \quad \text{(Eq 30)}$$

Relative volume of oxidation, A, is equal to the ratio of the oxidized volume, V_{os}, in the splat to the splat volume, V_{sp}. For the disk splat with the radius, R, and thickness, b, $V_{os} = 4\pi R^2 \delta_{ox}$ and $V_{sp} = 4\pi R^2 b$. Then:

$$A = b^{-1}\Delta_{ox} \quad \text{(Eq 31)}$$

Consider estimations of the oxidation parameters in the case of HVOF spraying of the Cr_3C_2-NiCr powder when chromium oxide Cr_2O_3 is formed. Taking $t_s = 10^{-3}$ s, $b = 3$ μm, $q_{ms} = 3.6$ kg/(m^{2}s), $\rho = 7500$ kgm^{-3} and $\rho_{ox} = 5210$ kgm^{-3}, it is obtained from Eq 29 to 31 that $H = 0.016$ (1.6%), $\Delta_{ox} = 0.07$ μm (70 nm), and $A = 0.023$. It can be seen that under the conditions considered, the splat oxidation is less pronounced than that which takes place during particle flight at the spraying distance.

The characteristic thickness of the oxidized layer, Δ_{ox}, in the case of the regular disk splats is approximately two orders of magnitude less than the splat thickness. Turbulent mixing of the splat liquid phase causes more uniform distribution of oxides in the bulk volume of this phase (Fig. 9b), which leads to a decrease in the thermal diffusivity of the liquid phase that slows down solidification.

The diffusion of oxygen can also take place. The thickness, Δ_{sp}, of the layer of diffusion can be estimated by the formula:

$$\Delta_{sp} = (D_e t_s)^{1/2} \quad \text{(Eq 32)}$$

Taking $t_s = 10^{-5}$s and $D_e = 4 \times 10^{-9}$m^{2}s^{-1}, it is found from Eq 32 that $\Delta_{sp} = 0.2$ μm. Thus, the thickness of the diffusive layer is essentially greater than that of the oxidation layer. The relative difference, B_{sp}, between Δ_{sp} and Δ_{ox} ($B_{sp} = 1 - \Delta_{ox}/\Delta_{sp}$) gives the relative volume of the splat containing dissolved oxygen. For HVOF spraying of the Cr_3C_2-NiCr powder, $B_{sp} = 65\%$. Thus, the value of B_{sp} is the same order of magnitude as the value of B_p.

Oxidation contributes to the development of splashing, and the thickness of the splash splats formed could be the same order of magnitude as the value of the oxidized layer, δ_{sp}. In the case of noticeable splashing when the value of A could be of the order of unity, the coating would have a substantial quantity of oxides.

Formation of the coating structure and properties depends essentially on the velocities of the coating cooling and solidification which, in turn, depends on the thermal resistance of the coating, R_{sp}. In the case when the disk splats are developed, the value of R_{sp} is the sum of the thermal resistance of the oxidized layer, R_3, and that of the rest of the splat, R_4 (Fig. 9a): $R_{sp} = R_3 + R_4$, $R_3 = \Delta_{sp}\lambda_{ox}^{-1}$, and $R_4 = (b - \Delta_{sp})\lambda_p^{-1}$. The ratio $X = R_3/R_4$ has the form:

$$X = \lambda_p \iota[\lambda_{ox}(1 - \iota)]^{-1} \quad \text{(Eq 33)}$$

In the case, for example, of HVOF spraying of the Cr_3C_2-NiCr powder onto a mild steel substrate when the disk splats are formed and $b = 2$ μm and $\Delta_{sp} = 0.2$ μm, it can be shown from Eq 32 and 33 that $X = 0.035$. Thus, the thermal resistance of the oxidized layer in this case does not play any significant role. The situation changes when significant splashing occurs and thin splash splats are formed.

The splat initial temperature also plays an important role in the splat oxidation. An increase in this temperature accelerates the kinetics of oxidation and increases the time, t_s, of splat solidification due to an increase in the heat content of the splat. Both factors lead to an increase in splat oxidation.

4.3 Influence on Droplet Flattening

First consider an agglomerate composite particle consisting of small high-melting point oxides and a melted binding

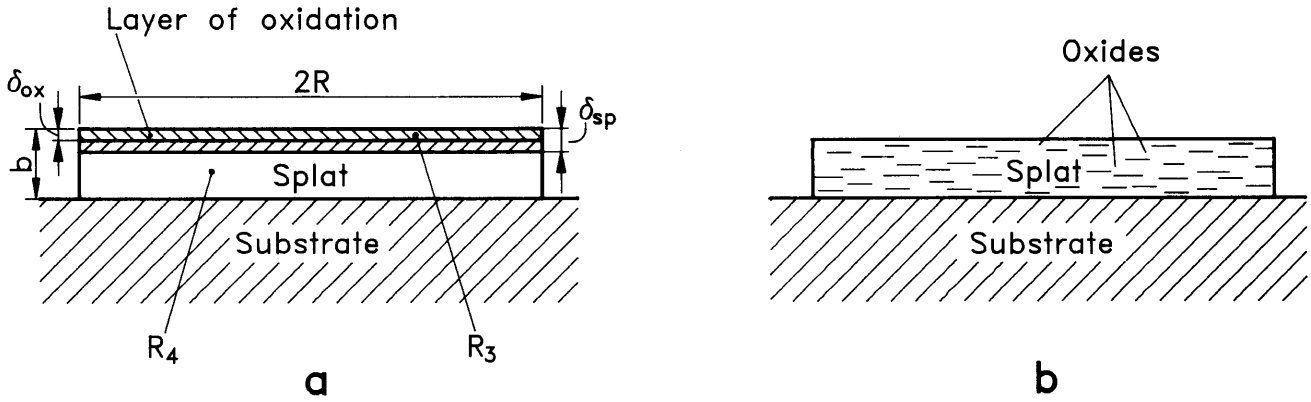

Fig. 9 Formation of layers of oxides and dissolved oxygen in a splat exposed to the oxygen-rich boundary layer enveloping the (a) splat and (b) mixing of the oxides in the bulk volume of the splat due to turbulence of the surrounding gases

metallic alloy. Such particles can be formed due to in-flight oxidation of an initial powder particle and mixing of the oxides with the melted binder. Assume that during thermal spraying this particle of radius, R_p, impinges normally with a velocity, U, onto the surface of a substrate or previously deposited coating layer and forms a cylindrical splat of radius, R, and thickness, b, which vary with time, t, during flattening. Assume further that the solid oxide components are significantly smaller than the splat thickness and that the surface roughness, ε_o, and a liquid-solid mixture of the impinging droplet can be considered as a quasi-homogeneous medium with a solid volume fraction, φ_1. Such a splat can also be formed from a powder particle, which had a regular surface layer of oxides destroyed during the droplet impingement onto the surface of the substrate.

When oxidation of the splat upper surface occurs, the oxides developed increase the oxide volume fraction $\varphi_1 = \varphi_{ox} + \iota_1$ of the liquid-solid mixture. Because the value of ι_1 is a function of time due to continuous formation of oxides in the liquid phase of the splat, the volume fraction, φ_1. is also a function of time: $\varphi_1 = \varphi_1(t)$. This is one of the main differences between the flattening of oxidized particles and that of composite powder particles consisting, for example, of carbides and a metallic binder (Ref 20).

An effective viscosity, μ_e, and an effective velocity of solidification, V_{se}, are introduced in the same manner as in Ref 20. Using the equations, methods, and ideas described in Section 3 and in Ref 14, 15, and 20 and taking into account that the Reynolds number $Re_e = 2R_pU\rho\mu_e^{-1}$, in thermal spraying is much more than unity ($Re_e >> 1$), the equations for the dimensionless transient values of the splat thickness, ζ, and radius, ξ, can be obtained. The formulas for the final values of the splat thickness, ζ_f, and radius, ξ_f, when $Re_e >> 1$ are similar to Eq 19 and 20, respectively.

The formulas discussed are similar to those for the flattening parameters of the composite powder particles, but they are more general and correspond to the case when the solid volume fraction, φ_1, can vary with time and the correction factor, $\psi < 1$. With an increase in the volume fraction of oxidation, the final splat thickness increases and the final splat radius decreases (Fig. 10).

It is seen that oxidation leads to an increase in the splat thickness and to a decrease in the splat radius due to an increase in the effective viscosity of the flattening droplet and a decrease in the velocity of solidification of the lower part of the splat.

The presence of dissolved oxygen causes a decrease in the contact wetting angle and, therefore, an improvement of wetting between the substrate and the flattening droplet (Ref 43). With an increase in the particle velocity at the spraying distance, the time of the particle flight decreases and the value of the time, t_{ox}, available for oxidation also decreases. Under such conditions, the volume fraction of oxidation, φ_{ox}, could be negligible; the value of B_p is about unity; and the main result of interaction of the molten particle with the surrounding oxygen could be its diffusion (dissolution) into the liquid particle material.

If in this case in-flight oxidation of the powder particle is the main contribution to the total volume fraction of oxidation, φ_1, and the value of B_{sp} is about unity, then in the final splat, there will be only dissolved oxygen that improves wetting between the splat and the substrate and contributes to an improvement of the substrate-splat adhesion. A similar situation can occur when the main contribution to oxidation arises from splat exposure to the surrounding oxygen-rich atmosphere. With an increase in the splat solidification velocity, the time of solidification, t_s, decreases and the volume fraction of oxidation in the splat, ι_1, can become negligible with that of the oxygen dissolution. Thus, the presence of dissolved oxygen can improve the quality of the coating.

4.4 *Effect on Splat-Substrate Mechanical Interaction*

Using the method and equations given in Ref 30, the formulas for the maximum pressure, P_m, developed upon droplet impact and its radial position, r_m, obtained, are similar to those presented in Ref 43. Because oxidation causes a decrease in the effective value of the Reynolds number, Re_e, due to an increase in the viscosity, μ_e, the value of r_m increases and the value of ΔP

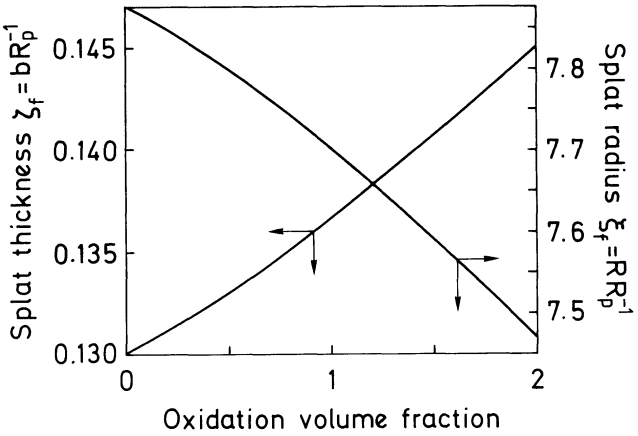

Fig. 10 Variation of the final values of the splat thickness and the splat radius with a volume fraction of oxidation. After Ref 42

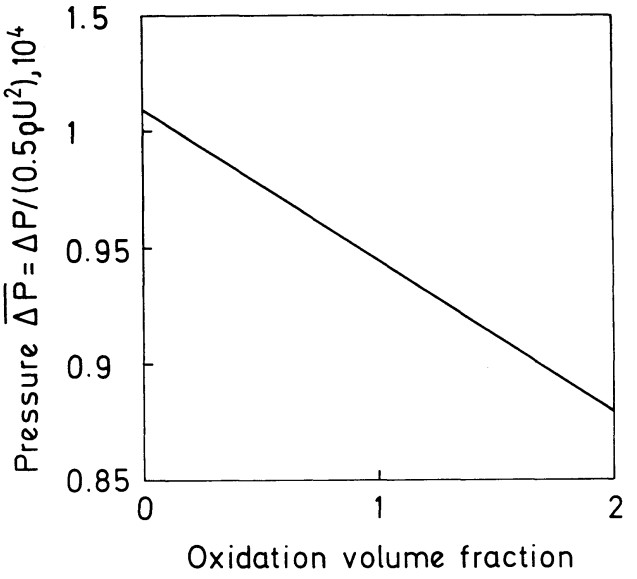

Fig. 11 Variation of pressure developed upon the droplet impact with a volume fraction of oxidation. After Ref 42

decreases. Therefore, the pressure developed during impact of an oxidized droplet is less than that formed when oxidation is absent. The behavior of ΔP is illustrated in Fig. 11 for plasma sprayed molybdenum particles when the time, t, is equal to the characteristic impact time, $t_c = R_p U^{-1}$ and $R_p = 20$ μm, $U = 150$ ms^{-1} $\rho = 9900$ kgm^{-3}, $\alpha = 0$, and $\beta = 0$. Thus, oxidation is detrimental to the substrate-coating adhesion.

In-flight interaction of the powder particle with oxygen may result not only in oxidation of the particle material but also in diffusion (dissolution) of oxygen in the liquid phase of the moving particle. The presence of the dissolved oxygen in the impinging droplet can decrease the surface tension coefficient, σ, and the contact wetting angle, τ, and this contributes to a decrease in splashing and in the capillary pressure. These factors favor improvement of splat-substrate mechanical interlocking. An important question, which remains to be answered, is whether their influence can overcome an effect of a decrease in the pressure developed upon the droplet impact due to oxidation that contributes to a decrease in the mechanical interlocking between the splat and the substrate.

From the results of Ref 44 and the formulas given in Ref 43, it follows that porosity increases with an increase in the surface tension coefficient, σ. Diffusion of oxygen causes a decrease in σ and, hence, a decrease in porosity. But because the value of ΔP exceeds markedly the capillary pressure, this factor is minor compared to the increase in the coating porosity.

4.5 Effect on Splat-Substrate Thermal Interaction

Oxidation decreases the pressure developed upon the droplet impact and the solidification velocity of the splat. Therefore, when the initial substrate temperature, T_{so}, is less than the transition temperature, T_{tr}, determining the splat morphology formed at droplet impact (Ref 45) ($T_{so} < T_{tr}$), the pressure developed could be not enough for the formation of of the supercooling ΔT_p associated with this pressure in the whole central part of the flattening droplet (Ref 43, 45). As a result, a regular disk splat could be developed only in the reduced area of the central part or, if the level of oxidation is high, splashing could occur everywhere.

With $T_{so} > T_{tr}$, the thermal supercooling that evolved was not enough for initiating solidification in the lower part of the whole splat. As a consequence, splashing could take place at the periphery of the flattening droplet and even in the central part.

Thus, oxidation is favorable for the development of splashing, and this is detrimental to the substrate-coating adhesion, as well as increasing the coating porosity. It seems that the negative effect of oxidation on the splat morphology and the coating properties may be weakened by an increase in the initial temperature of the substrate, at least for the relatively low levels of oxidation.

It should be mentioned that the presence of dissolved oxygen causes a decrease in the contact wetting angle and the coefficient of surface tension that contributes to a decrease in splashing.

4.6 Comparison with Experimental Data

The results obtained in Ref 35 indicate that coating oxidation decreases with an increase in the spraying distance when the influence of the heated products of combustion on the solidifying splat decreases and the splat solidification runs more rapidly. The results of Ref 35 also show that an increase in the splat initial temperature (which gives rise to the substrate temperature) leads to an increase in the coating oxidation.

Plasma spraying of yttria-stabilized zirconia powder onto steel and zirconia substrates demonstrated that surface splashing on the oxidized substrate always occured and splash splats were formed (Ref 46). This occurred in spite of the fact that the substrate initial temperature exceeded the critical temperature when regular disk splats were usually formed (Ref 45).

Experimental data established in Ref 47 for the parameters of flattening and solidification of splats formed after impingement of tin droplets onto a stainless steel substrate show that the contact wetting angle decreases with an increase in the substrate initial temperature.

An analytical expression for the maximum splat size derived in Ref 48 also shows that it increases with a decreasing contact angle of wetting. Finally, the results of modeling of the droplet flattening presented in Ref 11 and 48 show the influence of wetting between the substrate, and the flattening droplet on the droplet spreading on the substrate surface decreases with an increase in the velocity of the droplet impingement. The experimental data also show that the presence of dissolved oxygen in the liquid splat causes a decrease in the contact wetting angle (Ref 49).

Experimental data concerning HVOF spraying of stainless steel 316 on a mild steel substrate show that the level of oxidation increases with an increase in the spraying distance; at 0.3 m there is 12.49% of oxides in the coating, and at 0.45 m there is 25.66% of oxides (Ref 50). This supports a view that the main oxidation in this case occurs during the in-flight motion of the powder particles. A similar situation takes place during plasma spraying of stainless steel 431 on a mild steel substrate.

The coating structure obtained as a result of the HVOF spraying of the Cr_3C_2-NiCr powder onto a mild steel substrate shows that the formation of Cr_2O_3 seems to take place during the in-flight motion of the powder particles (Ref 39). This can be attributed to an increase in the particle residence time (and the value of t_{fl}) at the spray distance due to in-flight dissolution of Cr_3C_2 (Ref 39).

The experimental results show that during HVOF spraying of the Cr_3C_2-NiCr powder, the relative mass of chromium oxide in the coating is approximately 4.95% (Ref 51). Considering that oxidation occurs mainly during the in-flight motion of the powder particles, it is possible to estimate theoretically the level of oxidation as follows. The relative mass of oxidation, G, is equal to the ratio of the mass of the oxidized layer in the particle, m_{ox}, to the mass of the particle, m_p. Considering that $m_{ox} = \rho_{ox} V_{fl}$ and $m_p = \rho_p V_p$, then $G = 3\delta_{fl}\rho_{ox}(\rho_p R_p)^{-1}$, where ρ_p and ρ_{ox} are the densities of the particle and the oxide, respectively. From Ref 39 the value of t_{fl} is equal to 0.5 ms. Taking into account that the presence of carbides decreases the effective coefficient of diffusion of oxygen, $D_e = 10^{-9} m^2 s^{-1}$. Then, taking $R_p = 25$ μm, $\rho_p = 7800$ kgm^{-3} $\rho_{ox} = 5200$ kgm^{-3} and using Eq 27, the theoretical value of G is equal to 0.57 and is not far from the experimental value of $G = 0.495$.

Thus, the theoretical results agree well with the observed tendencies of oxidation and its influence on coating formation. The results obtained are also in agreement with the experi-

mental data, showing the effect of oxygen dissolved in the splat on wetting and with the experimental, analytical, and modeling results relating to the influence of wetting on the flattening parameters.

5. Conclusions

The formulas describing the time evolution of the splat thickness and radius in the flattening process during thermal spraying are established. The formulas take into account the surface roughness of the droplet impingement, the surface-splat friction, the splat solidification, and the loss of the droplet mass as a result of splashing and rebounding of the droplet material. Realistic correlations between the final values of the splat flattening parameters with the Reynolds number are obtained.

An equivalent dynamic viscosity of the liquid phase of the splat and an equivalent velocity of the droplet impingement are introduced, which account for the influence of the surface roughness and the surface-splat friction, as well as the splat solidification respectively on the droplet flattening during thermal spraying.

The splat thickness increases with an increase in the surface roughness and in the surface-splat friction and decreases when splat solidification takes place. The splat radius decreases with an increase in the surface roughness, the surface-splat friction, and the mass loss from the droplet. It increases when splat solidification occurs.

The approximate equations describing the time evolution of the thermally sprayed splat thickness and radius during flattening of the composite powder particles consisting of solid phase and binder are established, taking into account an increase in the particle viscosity and a decrease in the friction at the splat-substrate interface and in the velocity of solidification of the lower part of the splat. The realistic correlations between the final values of the splat thickness and splat radius and the Reynolds number are obtained, taking into account the mentioned phenomena. An effective dynamic viscosity of the splat liquid phase is introduced that accounts for the solid phase influence on the flow of the solid-liquid mixture during the droplet flattening.

A decrease in the powder particle radius leads to an increase in the level of the particle in-flight oxidation and the thickness of an oxidized layer. To decrease the particle in-flight oxidation, it is necessary to have a narrow size distribution of the powder particles with a relatively large mean value. Besides oxidation, diffusion of oxygen in the liquid phase of the particle occurs. The relative volume of oxygen diffusion and the thickness of the diffusive layer exceed markedly the similar values corresponding to the process of oxidation and also decrease with an increase in the particle radius. For the composite powder particles (e.g., consisting of carbides and a metallic binder), the level of oxygen diffusion is smaller than for a homogeneous particle without carbides. The oxidation behavior and diffusion of oxygen in the solidifying splat is similar to that in the moving particle.

Thermal resistance of the oxidized layer in the particle and in the splat increases with an increase in the particle thermal conductivity and the volume fraction of oxidation and a decrease in the thermal conductivity of the developed oxides. In the case of in-flight oxidation, this thermal resistance has the same order of magnitude as the total thermal resistance of the particle and plays an important role in the heat transfer processes. For the case of splat oxidation, the thermal resistance of the oxidized layer does not play any significant role when the regular disk splats are formed. This resistance becomes important when a significant splashing occurs and the thin splash splats are developed.

Flattening of the oxidized droplets impinging onto the substrate surface is similar to that of composite powder particles with an exception that the volume fraction of oxides varies with time. Oxidation leads to an increase in the splat thickness and a decrease in the splat radius.

Oxidation decreases the pressure developed upon the droplet impact and is detrimental to the mechanical contact between the substrate and the splat. Oxidation diminishes the contact heat transfer coefficient at the splat-substrate interface and the velocity of solidification of the splat. This leads to a decrease in the coating-substrate adhesion and an increase in the coating porosity.

Oxidation contributes to the development of splashing, which has a negative influence on the coating-substrate adhesion and increases the coating porosity. The negative effect of oxidation of the splat morphology and the coating properties seems to be alleviated by an increase in the initial temperature of the substrate.

A decrease in the contact wetting angle corresponding to an improvement of wetting between the splat and the substrate leads to a decrease in the splat thickness and an increase in the splat radius that contributes to reinforcement of the splat-substrate adhesive bonding. Influence of wetting on the flattening process decreases with an increase in the velocity of the droplet impingement onto the substrate surface and a decrease in the substrate initial temperature.

The results obtained agree well with the observed processes of flattening of droplets and the formation of splats in thermal spraying, enabling better understanding of these processes and predicting the parameters involved.

Acknowledgments

The authors would like to thank the Generalitat de Catalunya (project SGR 97-15) and CICYT (project MAT 96-0426) for financial support.

References

1. R.C. Dykhuizen, Review of Impact and Solidification of Molten Thermal Spray Droplets, *J. Therm. Spray Technol.*, Vol 3 (No. 4), 1994, p 351-361
2. R. McPherson, The Relationship between the Mechanism of Formation, Microstructure and Properties of Plasma Sprayed Coatings, *Thin Solid Films*, Vol 83, 1981, p 297-310
3. T. Watanabe, I. Kuribayashi, T. Honda, and A. Kanzawa, Deformation and Solidification of a Droplet on a Cold Substrate, *Chem. Eng. Sci.*, Vol 47 (No. 12), 1992, p 3059-3065
4. C. San Marchi, H. Liu, E.J. Lavernia, R.H. Rangel, A. Sickinger, and E. Muehlberger, Numerical Analysis of the Deformation and Solidification of a Single Droplet Impinging onto a Flat Substrate, *J. Mater. Sci.*, Vol 28, 1993 p 3313-3321
5. C.C. Berndt, W. Brindley, A.N. Goland, H. Herman, D.L. Houck, K. Jones, R.A. Miller, R. Neiser, W. Riggs, S. Sampath, M. Smith, and P. Spanne, Current Problems in Plasma Spray Processing, *J. Therm. Spray Technol.*, Vol 1 (No. 4), 1992, p 341-356

6. V.V. Sobolev, J.M. Guilemany, and A.J. Martín, Influence of Surface Roughness on the Flattening of Powder Particles during Thermal Spraying, *J. Therm. Spray Technol.*, Vol 5 (No. 2), 1996, p 207-214
7. H. Fukanuma, Mathematical Modeling of Flattening Process on Rough Surfaces in Thermal Spray, *Thermal Spray: Practical Solutions for Engineering Problems*, C.C. Berndt, Ed., ASM International, 1996, p 647-656
8. V.V. Sobolev, J.M. Guilemany, and A.J. Martín, Analysis of Splat Formation during Flattening of Thermally Sprayed Droplets, *Mater. Lett.*, Vol 29, 1996, p 185-190
9. V.V. Sobolev and J.M. Guilemany, Dynamic Processes during High Velocity Oxyfuel Spraying, *Int. Mater. Rev.*, Vol 41 (No. 1), 1996, p 13-32
10. V.V. Sobolev, J.M. Guilemany, and A.J. Martín, Investigation of Droplet Flattening during Thermal Spraying, *Surf. Coat. Technol.*, Vol 89, 1997, p 82-89
11. M. Pasandideh-Fard and J. Mostaghimi, Deformation and Solidification of Molten Particles on a Substrate in Thermal Plasma Spraying, *Thermal Spray Industrial Applications*, C.C. Berndt and S. Sampath, Ed., ASM International, 1994, p 405-414
12. M. Pasandideh-Fard and J. Mostaghimi, Droplet Impact and Solidification in a Thermal Spray Process: Droplet-Substrate Interactions, *Thermal Spray: Practical Solutions for Engineering Problems*, C.C.Berndt, Ed., ASM International, 1996, p 637-646
13. O.P. Solonenko, Advanced Thermodynamical Fundamentals of Melt Microdroplet Flattening and Solidification on a Substrate, *Thermal Spray Science and Technology*, C.C. Berndt and S. Sampath, Ed., ASM International, 1995, p 237-242
14. V.V. Sobolev and J.M. Guilemany, Influence of Solidification on the Flattening of Droplets during Thermal Spraying, *Mater. Lett.*, Vol 28, 1996, p 71-75
15. V.V. Sobolev and J.M. Guilemany, Flattening of Thermally Sprayed Particles, *Mater. Lett.*, Vol 22, 1995, p 209-213
16. V.V. Sobolev, J.M. Guilemany, and J.A. Calero, Substrate-Coating Thermal Interaction during High Velocity Oxy-Fuel (HVOF) Spraying, Part 1, Heat Transfer Processes, *Mater. Sci. Technol.*, Vol 11 (No. 8), 1995, p 810-819
17. J.M. Guilemany, V.V. Sobolev, J. Nutting, Z. Dong, and J.A. Calero, Thermal Interaction between WC-Co Coating and Steel Substrate in Process of HVOF Spraying, *Scr. Metall. Mater.*, Vol 31 (No. 7), 1994, p 915-920
18. V.V. Sobolev, J.M. Guilemany, J.A. Calero, and F.J. Villuendas, Heat Transfer between WC-Co Coating and Aluminum Alloy Substrate during High Velocity Oxygen-Fuel (HVOF) Spraying, *J. Therm. Spray Technol.*, Vol 4 (No. 4), 1995, p 408-414
19. V.V. Sobolev, J.M. Guilemany, and J.A. Calero, Substrate-Coating Thermal Interaction during High Velocity Oxy-Fuel (HVOF) Spraying, Part 2, Structure Formation, *Mater. Sci. Technol.*, Vol 11 (No. 10), 1995, p 1052-1059
20. V.V. Sobolev, J.M. Guilemany, and A.J. Martín, Flattening of Composite Powder Particles during Thermal Spraying, *J. Therm. Spray Technol.*, Vol 6 (No. 3), 1997, p 353-360
21. C. Moreau, P. Cielo, and M. Lamontagne, Flattening and Solidification of Thermally Sprayed Particles, *J. Therm. Spray Technol.*, Vol 1 (No. 4), 1992, p 317-323
22. T.W. Clyne, Numerical Treatment of Rapid Solidification, *Metall. Trans.*,Vol 15B, 1984, p 369-381
23. R. Ouziaux and J. Perrier, "Mecanique des Fluides Appliquée," tome 1, Dunod, Paris, 1972
24. S. Fantassi, M. Vardelle, A. Vardelle, and P. Fauchais, Influence of the Velocity of Plasma Sprayed Particles on Splat Formation, *J. Therm. Spray Technol.*, Vol 2 (No. 4), 1993, p 379-384
25. M. Vardelle, A. Vardelle, A.C. Leger, and P. Fauchais, *Thermal Spray Industrial Applications*, C.C. Berndt and S. Sampath, Ed., ASM International, 1994, p 555-562
26. C.J. Li, A. Ohmori, and Y. Harada, Effect of WC Particle Size on the Formation of HVOF Sprayed WC-Co Coatings, *Thermal Spraying—Current Status and Future Trends*, A. Ohmori, Ed., High Temp. Soc. Japan, 1995, p 235-240
27. R.G. Boothroyd, *Flowing Gas-Solids Suspensions*, Chapman and Hall Ltd., 1971, p 8-43
28. S.L. Soo, *Fluid Dynamics of Multiphase Systems*, Blaisdell, New York, 1967, p 133-276
29. V.V. Sobolev and P.M. Trefilov, *Thermophysics of Metal Solidification during Continuous Casting*, Metallurgy, Moscow, 1988, p 25-65
30. V.V. Sobolev and J.M. Guilemany, Droplet-Substrate Impact Interaction in Thermal Spraying, *Mater. Lett.*, Vol 28, 1996, p 331-335
31. V.V. Sobolev, J.M. Guilemany, and J.A. Calero, Dynamic Processes during In-Flight Motion of Cr_3C_2-NiCr Powder Particles in High Velocity Oxy-Fuel (HVOF) Spraying, *J. Mater. Process. Manuf. Sci.*, Vol 4 (No. 1), 1995, p 25-39
32. V. Palka, M. Brezovsky, J. Ivan, and J. Sith, Identification of Oxides in Plasma Sprayed APS Coating of the NiCrAlY Type, *Thermal Spray: International Advances in Coatings Technology*, C.C. Berndt, Ed., ASM International, 1992, p 537-542
33. L.N. Moskowitz, Application of HVOF Thermal Spraying to Solve Corrosion Problems in the Petroleum Industry, *Thermal Spray: International Advances in Coatings Technology*, C.C. Berndt, Ed., ASM International, 1992, p 611-618
34. T. Kraak, W. Herlaar, J. Wolke, K. de Groot, and E. Al Hydic, Jr., Influence of Different Gases on the Mechanical and Physical Properties of HVOF Sprayed Tungsten Carbide Cobalt, *Thermal Spray: International Advances in Coatings Technology*, C.C. Berndt, Ed., ASM International, 1992, p 153-158
35. C.M. Haskett and G.S. Settles, Turbulent Mixing of the HVOF Thermal Spray and Coating Oxidation, *Thermal Spray Industrial Applications*, C.C. Berndt and S. Sampath, Ed., ASM International, 1994, p 307-312
36. G.K. Creffield, M.A. Cole, and G.R. White, The Effect of Gas Parameters on HVOF Coatings, *Advances in Thermal Spray Science and Technology*, C.C. Berndt and S. Sampath, Ed., ASM International, 1995, p 291-301
37. P. Sahoo and G.W. Goward, On the Suitability and Application of MCrAlY Coatings under Various Operation Conditions, *Advances in Thermal Spray Science and Technology*, C.C. Berndt and S. Sampath, Ed., ASM International, 1995, p 539-544
38. A. Vardelle, P. Fauchais, and N.J. Themelis, Oxidation of Metal Droplets in Plasma Sprays, *Advances in Thermal Spray Science and Technology*, C.C. Berndt and S. Sampath, Ed., ASM International, 1995, p 175-180
39. V.V. Sobolev, J.M. Guilemany, and J.A. Calero, Influence of the Oxidation Process on the In-Flight Behaviour of Cr_3C_2-NiCr Powder Particles during High Velocity Oxy-Fuel (HVOF) Spraying, *Surface Modification Technologies XI*, T.S. Sudarshan, M. Jeandin, and K.A. Khor, Ed., Institute of Materials, London, 1998, p 86-90
40. V.V. Sobolev and J.M. Guilemany, Oxidation of Coatings in Thermal Spraying, *Mater. Lett.*, Vol 37, 1998, p 231-235
41. V.A. Efimov, Casting and Crystallisation of Steel, Metallurgy, Moscow, 1976, p 43-66 (in Russian)
42. V.V. Sobolev and J.M. Guilemany, Effect of Oxidation on Droplet Flattening and Splat-Substrate Interaction in Thermal Spraying, unpublished research, 1997, in press
43. V.V. Sobolev and J.M. Guilemany, Flattening of Droplets and Formation of Splats in Thermal Spraying: A Review of Recent Work, Part 2, *J. Therm. Spray Technol.*, 1998

44. V.V. Sobolev and J.M. Guilemany, Analysis of Coating Gas Porosity Development during Thermal Spraying, *Surf. Coat. Technol.*, Vol 70, 1994, p 57-68
45. V.V. Sobolev, Morphology of Splats of Thermally Sprayed Coatings, *Thermal Spray: Meeting Challenges of the 21st Century*, Vol 1, C. Coddet, Ed., ASM International, 1998, p 507-510
46. A.C. Leger, M. Vardelle, A. Vardelle, P. Fauchais, S. Sampath, C.C. Berndt, and H. Herman, Plasma Sprayed Zirconia: Relationships between Particle Parameters, Splat Formation and Deposit Generation—Part 1: Impact and Solidification, *Thermal Spray: Practical Solutions for Engineering Problems*, C.C. Berndt, Ed., ASM International, 1996, p 623-628
47. R. Bhola and S. Chandra, Splat Solidification of Tin Droplets, *Thermal Spray: Practical Solutions for Engineering Problems*, C.C. Berndt, Ed., ASM International, 1996, p 657-663
48. M. Pasandideh-Fard, Y.M. Qiao, S. Chandra, and J. Mostaghimi, Capillary Effects during Droplet Impact on a Surface, *Phys. Fluids*, Vol 8, 1996, p 650-659
49. N. Eustathopoulos and B. Drevet, Mechanisms of Wetting in Reactive Metal/Oxide Systems, in Proc. Mater. Res. Symp., *Mater. Res. Soc.*, Vol 314, 1993, p 15-26
50. V.V. Sobolev, J.M. Guilemany, and A.J. Martín, Influence of Mechanical and Thermal Behaviour of Stainless Steel Powder Particles during High Velocity Oxy-Fuel (HVOF) Spraying on Properties of Coatings, *Thermal Spray: Meeting the Challenges of the 21st Century*, C. Coddet, Ed., ASM International, 1998, p 503-506
51. J.A. Calero, Characterisation of Cermet Coatings of Cr_3C_2-NiCr Obtained by HVOF Spraying and Interpretation of Process Phenomenology by Mathematical Modelling, Ph.D. Thesis, University of Barcelona, 1997